Numerical evaluation of the viscoelastic and viscoplastic behavior of composites

G. Haasemann, V. Ulbricht

This paper is concerned with the development of homogenization methods in order to obtain the effective material parameters of viscoelastic and viscoplastic composites. In the case of a viscoelastic behavior, the constitutive laws at the heterogeneous scale are transposed into a LAPLACE-CARSON domain where the equations become similar to those of linear elasticity and classical homogenization procedures can be applied. Afterward, the results have to be converted by an inverse transformation. Mostly, this procedure is combined with analytical or semi-analytical models such as the self-consistent or Mori-Tanaka model. Since the application of this approach is limited to simple structured composites it is not suitable for materials with a complex internal architecture. In order to avoid this limitation, this paper is focused on the development of a homogenization procedure which is based on the LAPLACE-CARSON transformation and a numerical solution of the field problem. For heterogeneous material with viscoplastic or nonlinear viscoelastic properties, an additional linearization step is required. A new algorithm is proposed in order to combine this affine formulation with the numerical homogenization method.
Finally, these procedures are used to estimate the effective material behavior of different types of composites. With that, the accuracy of the results and efficiency of the methodologies is assessed.

1 Introduction

An increasing engineering application of heterogeneous materials such as composites demands for efficient modeling and simulation techniques based on the finite element method. For the investigation of the material stressing in a macroscopic problem, the FE-modeling of the heterogeneous micro-structure would be an extremely laborious task. Moreover, in most cases the time required to solve the resultant numerical problem will exceed any reasonable limit. Thus for the simulation it is a common practice to replace the heterogeneous material by a homogeneous equivalent medium (HEM). This in turn requires the identification of effective material properties which will be assigned to this HEM. In order to prevent expansive experimental investigations, homogenization methods can be used to obtain these material parameters.

In general there exists a wide range of different homogenization methods which can be subdivided into two groups depending on whether the solution is obtained analytically or numerically. As shown in the subsequent Section, the major advantage of numerical homogenization methods is the versatile application. This means the approach is independent of the microscopic structure and thus can be used to estimate the effective material properties of textile reinforced composites as well as honeycomb structures, for instance (Haasemann et al. (2009); Takano et al. (1995)). The computation of linear elastic material parameters based on this method is straightforward and widely used (Haasemann et al. (2006)). However, in the case of a nonlinear problem there is no unique approach. One of the most flexible solution is the FE^2-method where the stress state and tangent stiffness required in a structural simulation are obtained by the solution of a microscopic FE-model (Haasemann (2008); Miehe and Koch (2002)). Since this method is associated with an iterative algorithm, the numerical effort is significantly high. On the other hand, most analytical homogenization methods such as the self-consistent model or Mori-Tanaka-model are focused on a particular micro-structural configuration which results in a very high computational efficiency (Mori and Tanaka (1973); Hill (1965)). However, this also means that these methods can be applied only to this one type of composite.

The quest for analytical homogenization methods and the development of enhanced solutions is a subject for research since a long time. Thus the number of related publications is very high. The comparison of analytical and numerical homogenization techniques raises the question, whether there exists the possibility to combine both methods in order to take advantage of all favorable properties and to eliminate at least some shortcomings. Based on these considerations, this paper presents one approach for a linear viscoelastic material in Section 3 and another for a viscoplastic or nonlinear viscoelastic material in Section 4. All studies here are restricted to the small strain

assumption. For both methods and according to the developments published in Masson and Zaoui (1999), the LAPLACE-CARSON transformation is used. In the case of a viscoplastic or nonlinear viscoelastic material law, an additional linearization step leads to an affine formulation. Some applications to composite materials will be presented in Section 5. Finally the paper is closed with a summary and outlook. But first of all, the subsequent Section gives a general review to existing homogenization methods and defines some notations.

2 A review to existing homogenization methods

2.1 Coupling of state variables between different scales

A fundamental subject of all homogenization methods is concerned with the transition of some state variables such as stress or strain from the heterogeneous micro scale into the homogeneous macro scale. As proposed by Hill (1963), this coupling is based on the volume averaging denoted by

$$\langle \cdots \rangle := \frac{1}{|\mathcal{V}|} \int_{\mathcal{V}} \cdots dV \quad . \tag{1}$$

The definition of the domain $\mathcal{V} \subset \mathcal{R}^3$ depends on the homogenization method and the properties of the heterogeneous medium. In view of the textile reinforced composites, this domain is consistent with a unit cell which is a special case of a representative volume element (RVE). Applying the equation (1) to the heterogeneous stress field $\boldsymbol{\sigma}(\mathbf{y})$ and strain field $\boldsymbol{\varepsilon}(\mathbf{y})$ with $\mathbf{y} \in \mathcal{V}$ and assuming a microscopic equilibrium $\nabla \cdot \boldsymbol{\sigma} = \mathbf{0}$, the macroscopic stress $\boldsymbol{\Sigma}$ and strain $\mathbf{E}$ is given by

$$\boldsymbol{\Sigma} := \langle \boldsymbol{\sigma} \rangle = \frac{1}{|\mathcal{V}|} \int_{\partial \mathcal{V}} \mathbf{t} \otimes \mathbf{y} \, dA \quad \text{and} \quad \mathbf{E} := \langle \boldsymbol{\varepsilon} \rangle = \frac{1}{2|\mathcal{V}|} \int_{\partial \mathcal{V}} (\mathbf{u} \otimes \mathbf{n} + \mathbf{n} \otimes \mathbf{u}) \, dA \quad . \tag{2}$$

Here, $\mathbf{t} := \boldsymbol{\sigma}^T \cdot \mathbf{n}$ is the traction field at the boundary $\partial \mathcal{V}$, $\mathbf{n}$ - the outward normal and $\mathbf{u}$ - the displacement vector. One important property of both relations given in equation (2) is the possibility to change the volume into a surface integral. This is the foundation for the definition of boundary conditions in order to represent a desired macroscopic stress or strain state.

2.2 The Mori-Tanaka model

Beside the self-consistent model, the Mori-Tanaka model is a typical example for an analytical homogenization method (Mori and Tanaka (1973)). In general, this model is applied to a composite which consists of dilute inclusions distributed in a matrix material (Figure 1).
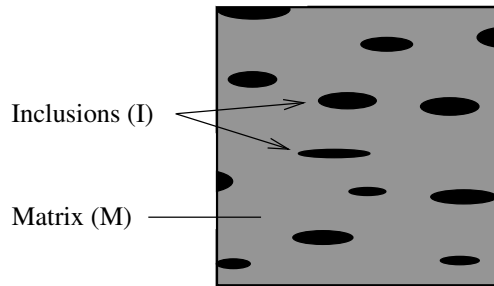
Figure 1. Dilute inclusions in a matrix

The derivation of the equations to compute a macroscopic stiffness tensor $\mathbf{C}$ is based on the assumption, that the state of each inclusion is equivalent to that of the inclusion alone in the matrix material. After the incorporation of the solution of Eshelby's problem, which is known explicitly for an ellipsoidal inclusion, the homogeneous strain inside the inclusion is given by

$$\varepsilon^I = \mathbf{A}^I : \mathbf{E} \tag{3}$$

where $\mathbf{A}^I$ is a strain concentration tensor (Nemat-Nasser and Hori (1993)). If all inclusions have the same orientation and the material properties $\mathbf{c}^I$ and $\mathbf{c}^M$ of inclusion and matrix, respectively, are isotropic, the macroscopic stiffness tensor can be obtained by

$$\mathbf{C} = \mathbf{c}^M + \chi(\mathbf{c}^I - \mathbf{c}^M) : \mathbf{A}^I \tag{4}$$

where χ is the volume fraction of inclusions.

As can be recognized by these relations, the Mori-Tanaka model provides a very efficient approach to compute the effective material properties. However, the application to nonlinear problems may lead to the violation of some requirements. One problem is concerned with the distribution of material properties which is assumed to be constant within each phase. Depending on the constitutive relations, the instantaneous stiffness which may by characterized by a tangent or secant operator, for instance, is changing locally. Thus the distribution of the respective material tensor is heterogeneous and this in turn is hard to be captured without any neglect in the framework of the Mori-Tanaka model.

Furthermore, the model described in this Section assumes an isotropic stiffness tensors for the constituents of the composite. But in the case of elasto-plastic materials, the tangent operator becomes anisotropic even if the constitutive relations are isotropic. Although this problem can be addressed by an extraction of the isotropic part (see e.g. Castañeda (1996) or Pierard and Doghri (2006)), there is still an uncertainty regarding the accuracy of the results.

As already mentioned in Section 1, the application of the Moria-Tanaka model is limited to composites with ellipsoidal inclusions. Depending on their aspect ratio, it is possible to compute the effective material properties of an infinite long inclusion. With respect to fiber reinforced materials, this model describes an unidirectional composite. However, textile reinforcements such as knitted or woven fabrics possess a more complex geometrical architecture and can not be investigated based on these analytical homogenization methods.

2.3 Homogenization based on the HILL-MANDEL condition

The definition of a heterogeneous micro structure including the respective constitutive relations and the computation of macroscopic quantities as described in Section 2.1 can be considered as part of a boundary value problem which lacks of boundary conditions. These can be derived based on the HILL-MANDEL condition. It states the equivalence of the averaged microscopic and macroscopic stress power (Hill (1967); Mandel (1964)). It follows, that

$$\langle \boldsymbol{\sigma} : \dot{\boldsymbol{\varepsilon}} \rangle = \langle \boldsymbol{\sigma} \rangle : \langle \dot{\boldsymbol{\varepsilon}} \rangle \quad . \tag{5}$$

There are three different types of boundary conditions which fulfill this assumption. These are:

- Linear velocities $\dot{\mathbf{u}}(\mathbf{y}) = \dot{\mathbf{E}} \cdot \mathbf{y} \quad \forall \quad \mathbf{y} \in \partial\mathcal{V}$,

- Constant tractions $\mathbf{t}(\mathbf{y}) = \boldsymbol{\Sigma} \cdot \mathbf{n}(\mathbf{y}) \quad \forall \quad \mathbf{y} \in \partial\mathcal{V}$ and

- Periodic velocities $\dot{\mathbf{u}}(\mathbf{y}^+) - \dot{\mathbf{u}}(\mathbf{y}^-) = \dot{\mathbf{E}} \cdot (\mathbf{y}^+ - \mathbf{y}^-)$ and
  anti-periodic tractions $\mathbf{t}(\mathbf{y}^+) + \mathbf{t}(\mathbf{y}^-) = 0 \quad \forall \quad \mathbf{y}^{+/-} \in \partial\mathcal{V}^{+/-} \quad .$

Here the surface $\partial\mathcal{V}$ of the RVE is subdivided into $\partial\mathcal{V}^+$ and $\partial\mathcal{V}^-$ according to their normal orientation. In comparison to each other, it is well known that the periodic boundary conditions provide the best approximation of effective material properties.

To obtain a solution of the boundary value problem defined by this homogenization theory, the finite element method can be used. If the material properties are linear elastic, it is possible to evaluate the macroscopic elasticity tensor $\mathbf{C}$ directly. In the case of a nonlinear material behavior, the FE^2-method can be applied. For this, the homogenization of the RVE-model provides the required stress and tangent stiffness at each integration point in a macroscopic FE-model (Haasemann et al. (2009); Miehe and Koch (2002); Kouznetsova (2002)).

In general, the evaluation of the homogenization method based on the HILL-MANDEL condition shows, that there are no limits regarding material properties at the micro scale and RVE-architecture. However, due to the iterative algorithm, the solution of a nonlinear material problem based on the FE^2-method is associated with a high numerical effort.

3 Homogenization of a linear viscoelastic composite

The determination of effective viscoelastic material properties based on the Mori-Tanaka model and the correspondence principle has been investigated by Pierard et al. (2004). In order to avoid the disadvantages as summarized in 2.2, this Section describes a similar approach in combination with the numerical homogenization procedure of Section 2.3.

3.1 Viscoelastic constitutive equations

The constitutive relations of a multiple-parameter linear viscoelastic body are derived from a parallel model. It consists of an HOOKEan spring of stiffness $\mathbf{G}_\infty$ and n_{mw} MAXWELL elements of stiffness $\mathbf{G}_j$ and viscosity $\boldsymbol{\eta}_j$. Supposing a relaxation time τ_j defined by $\frac{1}{\tau_j}\mathbf{I} = \mathbf{G}_j : \boldsymbol{\eta}_j^{-1}$ which is independent of any orientation, the linear rate equations of MAXWELL-element j are given by

$$\dot{\mathbf{h}}_j + \frac{1}{\tau_j}\mathbf{h}_j = \mathbf{G}_j : \dot{\boldsymbol{\varepsilon}} \tag{6}$$

where $\mathbf{h}_j$ is the viscoelastic stress variable. Applying the integration factor method, the solution of equation (6) can be written as

$$\mathbf{h}_j = \mathbf{G}_j \int\limits_{-\infty}^{t} \dot{\boldsymbol{\varepsilon}}(u)\, \mathrm{e}^{-\frac{t-u}{\tau_j}}\, du \quad . \tag{7}$$

According to the parallel connection of HOOKEan spring and MAXWELL elements, the total stress tensor $\boldsymbol{\sigma}$ is defined by $\boldsymbol{\sigma} = \boldsymbol{\sigma}_\infty + \sum_{j=1}^{n_{\mathrm{mw}}} \mathbf{h}_j$ where $\boldsymbol{\sigma}_\infty := \mathbf{G}_\infty : \boldsymbol{\varepsilon}$. Assuming $\boldsymbol{\varepsilon}(t) = \mathbf{0} \quad \forall \quad t < 0$, the constitutive relations for this linear viscoelastic material model can be expressed as

$$\boldsymbol{\sigma}(t) = \mathbf{G}(t) : \boldsymbol{\varepsilon}(t=0) + \int\limits_{0}^{t} \mathbf{G}(t-u) : \dot{\boldsymbol{\varepsilon}}(u)du = \mathbf{G}(t) : \boldsymbol{\varepsilon}(t=0) + [\mathbf{G} * \dot{\boldsymbol{\varepsilon}}](t) \quad , \tag{8}$$

where the operator $[\,*\,]$ denotes the convolution integral and the tensorial relaxation function $\mathbf{G}(t)$ is defined as

$$\mathbf{G}(t) = \mathbf{G}_\infty + \sum_{j=1}^{n_{\mathrm{mw}}} \mathbf{G}_j\, \mathrm{e}^{-\frac{t}{\tau_j}} \quad . \tag{9}$$

3.2 Correspondence principle

The elastic-viscoelastic correspondence principle provides the possibility to convert the linear rate-dependent material law (8) into transformed equations which are formally equivalent to those of a linear elastic solid (Alfrey (1944)). This analogy can be derived by applying the LAPLACE transformation. Alternatively, the LAPLACE-CARSON transformation, defined by

$$f(t) \circ\!\!-\!\!\bullet f^*(s) := \mathcal{L}[f(t)]_s = s \int\limits_{0}^{\infty} f(t)\, \mathrm{e}^{-st}dt \quad , \tag{10}$$

can be used. The main advantage of this transformation lies in the unchanged dimension of the function in the LAPLACE and time domain. Since the convolution integral in equation (8) reduces to a contraction under this transformation, it follows

$$\boldsymbol{\sigma}(t) = \mathbf{G}(t) : \boldsymbol{\varepsilon}(t=0) + \mathbf{G}(t) * \dot{\boldsymbol{\varepsilon}}(t) \circ\!\!-\!\!\bullet \boldsymbol{\sigma}^*(s) = \mathbf{G}^*(s) : \boldsymbol{\varepsilon}^*(s) \quad . \tag{11}$$

These constitutive equations in the LAPLACE domain are similar to that of a linear elastic material except that there is a dependence on the LAPLACE variable s.

3.3 Homogenization algorithm

The LAPLACE-CARSON transformation of the boundary value problem given by the homogenization method according to Section 2.3 can be used to compute an effective relaxation tensor in the LAPLACE domain. The associated algorithm is illustrated in Figure 2.
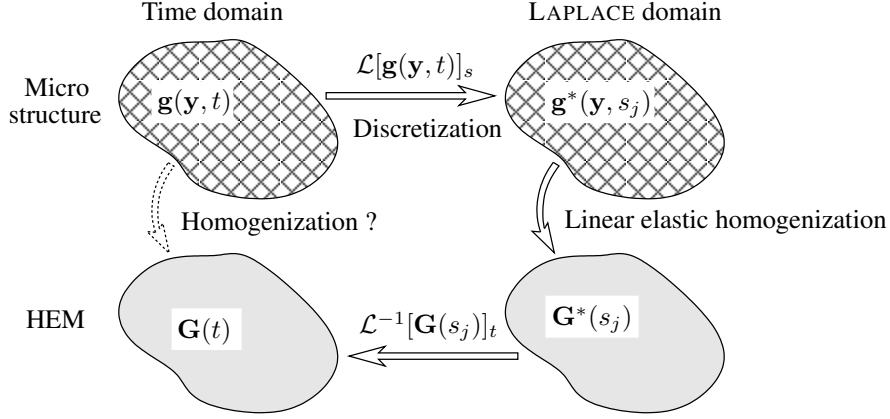
Figure 2. Homogenization based on elastic-viscoelastic correspondence principle

The starting point is a heterogeneous micro structure with known viscoelastic material properties $\mathbf{g}(\mathbf{y}, t)$ in the time domain. Since there is no unique and direct homogenization procedure to obtain the effective relaxation tensor $\mathbf{G}(t)$ of a HEM, the time domain is exchanged with the LAPLACE domain. Thereby, the numerical implementation requires a discretization of the LAPLACE variable s. For each parameter s_j and for all material constituents of the micro structure, the image functions $\mathbf{g}^*(\mathbf{y}, s_j)$ have to be computed. Within the application of the FEM, these material properties are assigned to respective finite elements. The solution of all boundary value problems defined by the homogenization method gives a set of effective relaxation tensors $\mathbf{G}^*(s_j)$. In order to obtain the material properties in the time domain, an inverse LAPLACE-CARSON transformation, denoted by $\mathcal{L}^{-1}[\ldots]_t$, is required. The numerical algorithm to perform this operation is summarized in Appendix A. The ansatz used for this method can be expressed as rank-2 tensor function by

$$\mathbf{f}(t) = \mathbf{A} + \mathbf{B}t + \sum_{j=1}^{n_{max}} \mathbf{b}_j (1 - e^{-\frac{t}{\tau_j}}) \quad . \tag{12}$$

Since we assume a state of equilibrium as time tends to infinity, the linear part is eliminated by setting $\mathbf{B} = 0$. The tensors $\mathbf{A}$ and $\mathbf{b}_j$ are computed according to the procedure described in Appendix A. Finally, by comparison of equation (12) with (9), it follows that

$$\mathbf{G}_j = -\mathbf{b}_j \quad \text{and} \quad \mathbf{G}_\infty = \mathbf{A} + \sum_{j=1}^{n_{max}} \mathbf{b}_j \quad . \tag{13}$$

With that, the effective relaxation function $\mathbf{G}(t)$ of the HEM is known and can be used in a simulation of a macroscopic structural problem.

This homogenization algorithm can be applied to any configuration of a micro structure as long as the material properties of the constituents are linear elastic or viscoelastic. In comparison to the FE^2-method, this approach does not require an iterative solution technique and thus is characterized by a high computational efficiency.

4 Homogenization of viscoplastic composites

In this Section, composite materials with viscoplastic material properties are considered. Due to the loading path dependent and in most cases anisotropic properties, it is extremely difficult to find a macroscopic material law which represents the effective behavior entirely. But this would be required if the homogenization step should remain separate from a macroscopic simulation. Otherwise, a coupled simulation such as the FE^2-method does not necessitate a pre-definition of macroscopic constitutive relations. Furthermore, Masson and Zaoui (1999) have presented an affine formulation which makes use of the self-consistent estimates. In the following, this affine formulation is combined with the LAPLACE-CARSON transformation and the numerical homogenization technique.

4.1 Viscoplastic constitutive equations

In view of the specific application given in Section 5.2, this Subsection gives a summary of the basic equations of a viscoplastic model. The rate-dependent plastic material law considered here is named after Perzyna (1963) and

presents the feature of an elastic domain where the linear elastic constitutive relations are given by

$$\dot{\boldsymbol{\sigma}} = \mathbf{C} : (\dot{\boldsymbol{\varepsilon}} - \dot{\boldsymbol{\varepsilon}}^{vp}) \quad . \tag{14}$$

According to the associative plasticity, the viscoplastic strain rate $\dot{\boldsymbol{\varepsilon}}^{vp}$ can be computed with the plastic flow rule

$$\dot{\boldsymbol{\varepsilon}}^{vp} = \frac{\langle g(f) \rangle}{\eta} \frac{\partial f(\boldsymbol{\sigma}, \alpha)}{\partial \boldsymbol{\sigma}} \tag{15}$$

where the MCCAULEY brackets $\langle \ldots \rangle$ are defined as $\langle g \rangle := (g + |g|)/2$. The yield function $f(\boldsymbol{\sigma}, \alpha)$ depending on the current stress state $\boldsymbol{\sigma}$ and the accumulated plastic strain α is given by

$$f(\boldsymbol{\sigma}, \alpha) = \sqrt{\frac{3}{2}} \|\boldsymbol{\sigma}\| - \sigma_y - R(\alpha) \tag{16}$$

with a yield stress σ_y and a hardening function $R(\alpha)$ which is chosen according to the respective material behavior. By taking Norton's power law to specify the creep function g used in equation (15), it follows

$$g(f) = \sigma_y \left(\frac{f(\boldsymbol{\sigma}, \alpha)}{\sigma_y} \right)^m \quad , \tag{17}$$

where the relaxation exponent m is a material property.

4.2 Affine formulation

In a first step, the constitutive equations such as given in Section 4.1 are linearized at a time $t_n < t$. Then the equations for the viscoplastic strain rate and hardening rate read

$$\begin{aligned}
\dot{\boldsymbol{\varepsilon}}^{vp}(t) &= \dot{\boldsymbol{\varepsilon}}^{vp}(t_n) + \mathbf{m}(\tau) : [\boldsymbol{\sigma}(t) - \boldsymbol{\sigma}(t_n)] + \mathbf{n}(\tau) [\alpha(t) - \alpha(t_n)] \quad \text{and} \\
\dot{\alpha}(t) &= \dot{\alpha}(t_n) + \mathbf{p}(\tau) : [\boldsymbol{\sigma}(t) - \boldsymbol{\sigma}(t_n)] + q(\tau) [\alpha(t) - \alpha(t_n)] \quad ,
\end{aligned} \tag{18}$$

where the components of the tangent tensors $\mathbf{m}(\tau)$, $\mathbf{n}(\tau)$, $\mathbf{p}(\tau)$ and $q(\tau)$ evaluated at τ with $t_n \leq \tau \leq t$ are defined by

$$m_{ijkl}(\tau) := \left. \frac{\partial \dot{\varepsilon}_{ij}}{\partial \sigma_{kl}} \right|_{\tau} \quad , \quad n_{ij}(\tau) := \left. \frac{\partial \dot{\varepsilon}_{ij}}{\partial \alpha} \right|_{\tau} \quad , \quad p_{ij}(\tau) := \left. \frac{\partial \dot{\alpha}}{\partial \sigma_{ij}} \right|_{\tau} \quad \text{and} \quad q(\tau) := \left. \frac{\partial \dot{\alpha}}{\partial \alpha} \right|_{\tau} \quad . \tag{19}$$

As it is shown by Masson and Zaoui (1999), the solution of the linearized equations is given by

$$\dot{\boldsymbol{\varepsilon}}(t) = \frac{d}{dt} \left[\int_0^t \mathbf{S}_\tau(\tau, t - u) : \dot{\boldsymbol{\sigma}}(u) du \right] + \dot{\boldsymbol{\varepsilon}}^0(\tau, t) = \frac{d}{dt} \left[\mathbf{S}_\tau * \dot{\boldsymbol{\sigma}} \right](\tau, t) + \dot{\boldsymbol{\varepsilon}}^0(\tau, t) \tag{20}$$

where the relations to compute the compliance tensor $\mathbf{S}_\tau$ and the eigenstrain rate $\dot{\boldsymbol{\varepsilon}}^0(\tau, t)$ adapted to the constitutive law described in Section 4.1 can be found in Appendix B.
Changing the equations (20) to express the stress as function of strain, it can be compared with the relations of (8). Due to the linearization procedure, the viscoplastic material law has transformed into a viscoelastic type problem with eigenstrain. Thus, in a second step, the LAPLACE-CARSON transformation is applied to equation (20) which results in the constitutive law

$$\boldsymbol{\varepsilon}^*(s) = \mathbf{S}_\tau^*(\tau, s) : \boldsymbol{\sigma}^*(s) + \boldsymbol{\varepsilon}^{0*}(\tau, s) \tag{21}$$

or equivalently

$$\boldsymbol{\sigma}^*(s) = \mathbf{C}_\tau^*(\tau, s) : \left[\boldsymbol{\varepsilon}^*(s) - \boldsymbol{\varepsilon}^{0*}(\tau, s) \right] \quad \text{with} \quad \mathbf{C}_\tau^* := (\mathbf{S}_\tau^*)^{-1} \quad , \tag{22}$$

where the details to $\mathbf{S}_\tau^*(\tau, s)$ and $\boldsymbol{\varepsilon}^{0*}(\tau, s)$ are reported in Appendix B.
The behavior described with equation (21) is formally equivalent to that of a thermoelastic material. However, the tensors denoted by $\boldsymbol{\sigma}^*(s)$ and $\boldsymbol{\varepsilon}^*(s)$ are just virtual stresses and strains, respectively. The computation of the real stress $\boldsymbol{\sigma}(t)$ and strain $\boldsymbol{\varepsilon}(t)$ requires again an inverse LAPLACE-CARSON transformation as described in Appendix A.

4.3 Affine homogenization algorithm

The affine homogenization scheme proposed by Masson and Zaoui (1999) considers a linearization step according to equation (19) with $t = t_n = \tau$. Then the mechanical response depends on itself and with that, this procedure becomes implicit. The solution documented in the cited publication is an iteration combined with the self-consistent model. Thereby, this algorithm starts with some estimates for the stress and accumulated plastic strain and it is finished if the deviation of these quantities between two consecutive steps is less than a convergence criteria. In view of the numerical homogenization method, this is an inappropriate procedure since it is hardly possible to obtain reasonable estimates for $\boldsymbol{\sigma}(\tau, \mathbf{y})$ and $\alpha(\tau, \mathbf{y})$. Thus, we introduce a modified algorithm which is illustrated schematically in Figure 3.
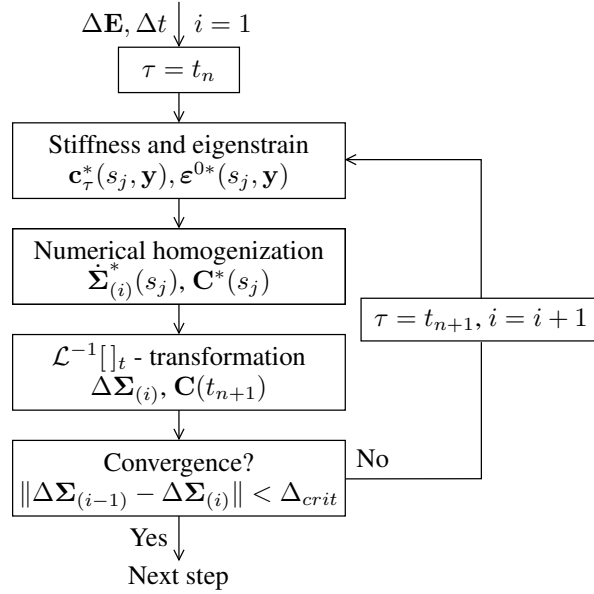
Figure 3. Affine homogenization algorithm

At first it is assumed, that there is a given macroscopic strain increment $\Delta \mathbf{E}$ related to a time increment Δt. The origin of these values can be a previously defined strain path or a structural FE-simulation. In the latter case, this affine homogenization algorithm is linked to the macroscopic FE-problem similar to the FE^2-method. Next we define a linearization time $\tau = t_n$ and with that, the following part of this algorithm becomes explicit. For the subsequent determination of the stiffness tensor $\mathbf{c}_\tau^*(s_j, \mathbf{y})$ and the eigenstrain $\varepsilon^{0*}(s_j, \mathbf{y})$, we need to know all state variables such as $\dot{\varepsilon}^{vp}$ or $\boldsymbol{\sigma}$ at the time step t_n. The integral expressions given in equation (33) (Appendix B) could lead to the assumption, that the entire stress and viscoplastic strain history must by available. However, the amount of data to be stored can be reduced if the domain of integration is subdivided additively into the intervals $[0, t_n]$ and $[t_n, t_n + \Delta t]$. With that, we just need to know the value of the integral on the first time domain which gets updated by the integral evaluated on the current time increment Δt.

Unlike the analytical homogenization methods, this algorithm allows for a noncontinuous distribution of the stiffness and strain inside the RVE. With the application of the FEM, the stiffness and eigenstrain has to be assigned to each integration point of all elements. The solution of the boundary value problem provides the macroscopic stress rate $\dot{\boldsymbol{\Sigma}}_{(1)}^*(s_j)$ and tangent stiffness $\mathbf{C}^*(s_j)$ where the subscript (1) indicates the first iteration. If the inverse LAPLACE-CARSON transformation is used subsequently, we obtain a stress increment $\Delta \boldsymbol{\Sigma}_{(1)}$ and the current tangent stiffness $\mathbf{C}(t_{n+1})$. In a final step, the norm of the stress increments $\|\Delta \boldsymbol{\Sigma}_{(i-1)} - \Delta \boldsymbol{\Sigma}_{(i)}\|$ is used as a convergence criterion as given in Figure 3. For the special case of this first iteration, the previous stress increment is defined by $\Delta \boldsymbol{\Sigma}_{(0)} = \langle \boldsymbol{\sigma}(\mathbf{y}) \rangle$ where the micro stress is computed according to the viscoplastic constitutive relations. If the material behavior has been purely elastic, both stress increments are equivalent within a tolerance of the numerical precision. On the other hand, with occurrence of a nonlinearity, the limit value Δ_{crit} will be violated and an iteration will start until this convergence criterion is met. In contrast to the first cycle, all iterations with $i > 1$ must be implicit in order to account for the change due to the nonlinear behavior. Thus the linearization time is determined by $\tau = t_{n+1}$.

In comparison to the FE^2-method, the advantage of this procedure lies in a lower computational effort. We observed a rather small number of iterations i. In general, this algorithm did not need more than two cycles. In view of the FE^2-method, the increasing length of a loading path of each integration point during the advance of a macroscopic simulation is transferred directly to the RVE-model. With that, the computational time required is

growing exceedingly. In contrast to that, the computational effort during a solution based on this numerical affine method remains almost constant. On the other hand, a disadvantage is the large number of data to be stored as well as an inadequacy of the numerical inverse LAPLACE-CARSON transformation. The latter subject will described more precisely in the subsequent Section 5.2.

5 Application to composite materials

5.1 Linear viscoelastic composites

5.1.1 Unidirectional composite

In order to investigate the accuracy of the homogenization method developed for linear viscoelastic composites, a structural problem as shown in Figure 4 is used.
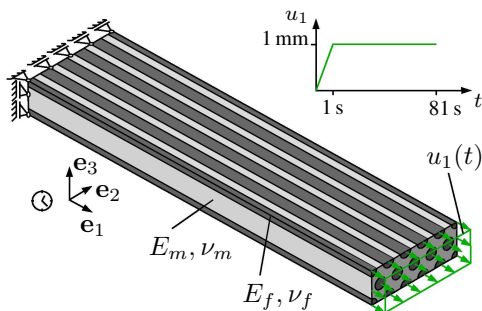
Figure 4. Beam model with UD composite
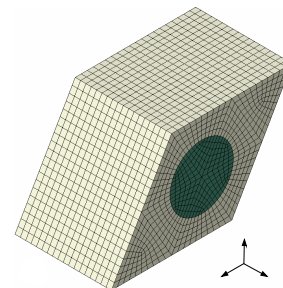
Figure 5. RVE of UD composite

A beam made of an unidirectional (UD) composite is fixed at one end and a given displacement $u_1(t)$ is applied at the other end. The isotropic material properties of the fiber and matrix material are given in Table 1. These values

	Fiber	Matrix
Modulus	$(70 + 200\,\mathrm{e}^{-\frac{t}{10s}})$	$(3 + 15\,\mathrm{e}^{-\frac{t}{1s}})$
POISSON's ratio	0.2	0.35

Table 1: Viscoelastic material properties of matrix and fiber material

indicate, that the stiffness of the fibers is much higher compared to the matrix material. The hexagonal arrangement of the fibers ensure a transversely isotropic material behavior at the macro scale. This gives the reason to define the shape of the RVE as parallelepiped where the FE-model is displayed in Figure 5. The homogenization according to Section 3 is carried out with 20 logarithmically spaced collocation points in the range of $s \in [10^{-3}, 10^3]$. The results in terms of effective material properties are assigned to elements of a homogeneous FE-model. Therefor, the implementation of an anisotropic viscoelastic law is required. Here, an algorithm as described by Kaliske (2000) is specified within the user-defined subroutine UMAT in ABAQUS/Standard (Abaqus (2008)).

To verify the results obtained with this homogeneous FE-model, a second simulation based on a heterogeneous model and equivalent boundary conditions is applied. The total reaction forces $F(t)$ of both models are compared in Figure 6. Since the deviations are less then 1%, we can conclude a good agreement of our results and a sufficiently high precision of this homogenization method.
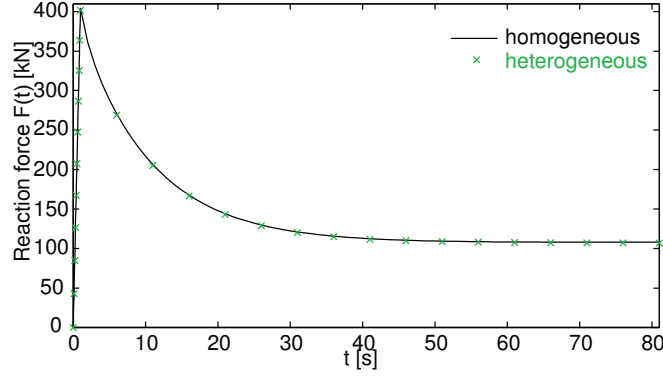
Figure 6. Reaction forces of UD-model

5.1.2 Textile reinforced composite with biaxial weft-knit

To illustrate the versatile utilization of the numerical viscoelastic homogenization method, it is applied to a textile reinforced composite. The fabric considered here is called biaxial weft-knit. As shown in Figure 7, it consists of layer-wise arranged warp and weft yarns. The weft knit holds these yarns tight together and prevents a decomposition of the fabric.
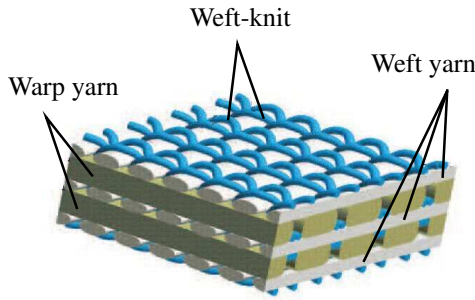
Figure 7. Biaxial weft-knit
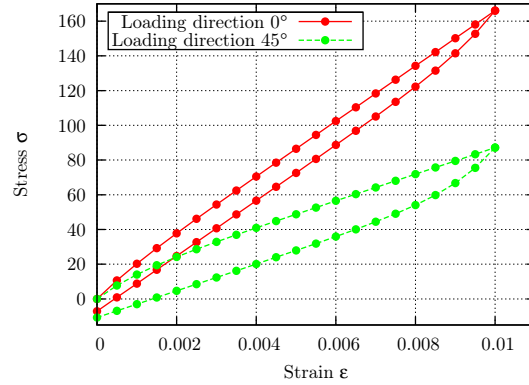
Figure 8. Macroscopic stress strain curves of an composite with biaxial weft-knit

The employment of this fabric as reinforcement for composites results in advantageous mechanical properties (Haasemann (2008)). For instance, all straight aligned yarns cause a high stiffness for the respective orientation and the weft-knit ensures a delamination resistance.

Since the generation of a FE-mesh based on conventional volume elements would be very laborious, we have used the Binary Model as an efficient modeling technique (Carter et al. (1994); Haasemann et al. (2006)). It consists of link elements with an axial stiffness defined by the yarn-matrix domain. The effective medium elements, which are volume elements, represent all other properties of the matrix material and the fibers. Since both element types are connected parallel, the modulus $e_{\mathrm{le}}(t)$ assigned to the link elements is given by

$$e_{\mathrm{le}}(t) = e_1^{\mathrm{UD}} - e_{\mathrm{ax}}^{\mathrm{EM}}(t) \quad \circ\!\!-\!\!\bullet \quad e_{\mathrm{le}}^*(s) = e_1^{\mathrm{UD}*} - e_{\mathrm{ax}}^{\mathrm{EM}*}(s) \quad , \tag{23}$$

where e_1^{UD} and $e_{\mathrm{ax}}^{\mathrm{EM}}(t)$ are the moduli of the real fiber-matrix domain and the associated volume element, respectively. Although we assume a linear elastic behavior of the fiber-matrix material, the value of e_{le} depends on the time t. The LAPLACE-CARSON transform of this material property is given on the right hand side in equation (23). $e_{\mathrm{le}}^*(s)$ is the modulus which has to be used for the homogenization method as described in Section 3.3.

As a result of this computation, Figure 8 shows two macroscopic stress-strain paths. Each curve in this diagram is the response of an uni-axial strain function

$$E(t) := \dot{E}\,t \quad \text{with} \quad \dot{E} := \begin{cases} +0.001 & \text{for} \quad 0 \le t/\mathrm{s} \le 10 \\ -0.001 & \text{for} \quad 10 \le t/\mathrm{s} \le 20 \end{cases} \tag{24}$$

In view of an orientation where $0°$ is aligned to the warp yarn, this strain is applied to the direction $0°$ and $45°$. Figure 8 shows the strong directional behavior of this type of composite. Due to the aligned yarns, the stiffness in

130

$0°$ and $90°$ is much higher than in $45°$. Similar, the viscose behavior is more significant in $45°$ since the fibers are assumed to be linear elastic without viscosity.

This example illustrates the general usability of the numerical viscoelastic homogenization method even in the case of a composites with a highly complex architecture at the micro or meso scale.

5.2 Homogenization of viscoplastic materials

This part presents the application of the numerical homogenization based on the affine formulation as described in Section 4.3. To investigate the general behavior, a homogeneous RVE represented by a FE-model is considered. The model has the shape of a rectangular cuboid with a constant edge length of $2\,\mathrm{mm}$. Referring to the notation introduced in Section 4.1, the viscoplastic material properties assigned to the RVE are: $\sigma_y = 60$, $m = 1$, $\eta = 300$ and $R(\alpha) = 2000\,\alpha$. According to Section 2.3, periodic boundary conditions are used to compute the homogenized tensors $\dot{\mathbf{\Sigma}}(s_j)$ and $\mathbf{C}^*(s_j)$ and the macroscopic strain path is chosen as given in equation (24).

A homogenization procedure applied to a homogeneous RVE is for all practical purposes unnecessary. However, as outlined subsequently, it gives the possibility to analyze the characteristics of local variables and the macroscopic behavior based on analytical solutions.

Figure 9 shows the macroscopic stress-strain response of the numerical homogenization as well as the analytical solution.
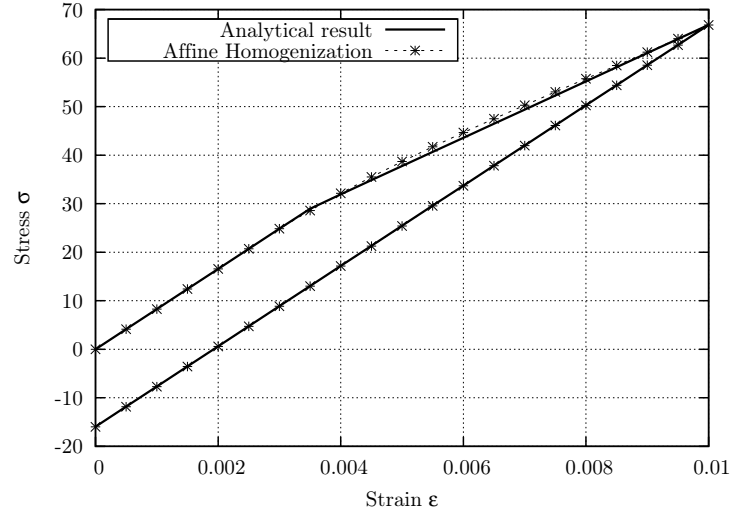
Figure 9. Macroscopic tress strain curves of a viscoplastic material

The comparison reveals a good agreement of both curves as long as the behavior is purely elastic. During the time period with a positive strain rate and with the initiation of viscoplastic effects, some small deviations can be recognized. These are caused by some limitations associated with the numerical inverse LAPLACE-CARSON transformation. In order to illustrate this problem, an ideal elastic-plastic material with modulus E and yield stress σ_y is subjected to a constant strain rate $\dot{\bar{\varepsilon}}$. In that case it is possible to derive all equations analytically. One result is the eigenstrain $\varepsilon^{0*}(\tau, s)$ which is known as function in the LAPLACE domain. The inverse transformation reveals the strain rate in the time domain as follows

$$
\begin{aligned}
\dot{\varepsilon}^0(t) \;=\;& \dot{\varepsilon}^{in}(t_n)H(t-t_n) - \dot{\bar{\varepsilon}}\left(H(t-t_y) - H(t-t_n)\right) - \mathbf{m}(\tau) : \left[E\dot{\bar{\varepsilon}}t\left(1 - H(t-t_y)\right) + \ldots\right. \\
& \left. \ldots + E\tau\left(H(t-t_y) - H(t-t_n)\right)\left(\dot{\bar{\varepsilon}}(1 - e^{-\frac{1}{\tau}(t-t_y)}) + \frac{\sigma_y}{E\tau}\right)\right] + \boldsymbol{\sigma}(t_n)H(t-t_n) \quad .
\end{aligned}
\tag{25}
$$

It can be recognized that the functional character is dominated by the HEAVISIDE step function H. With $t_n = \tau = 2$, the plot of $\dot{\varepsilon}^0(t)$ is shown in Figure 10 where we have a kink at $t = t_n$.
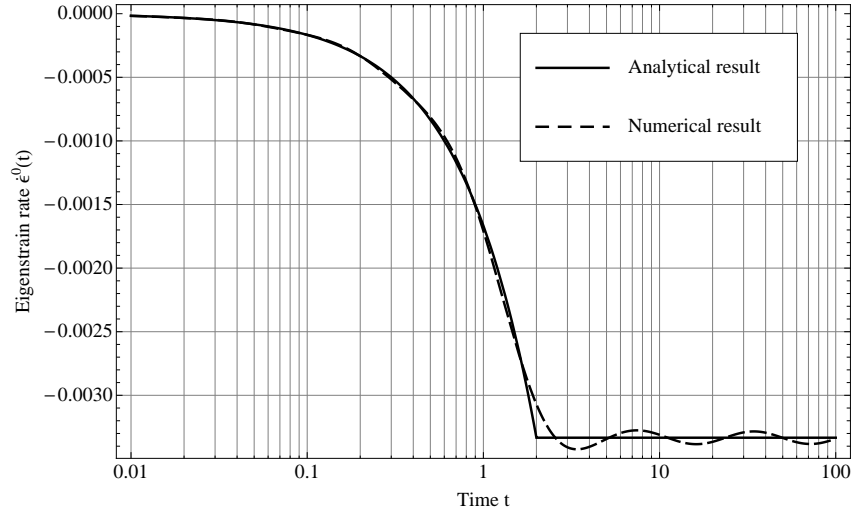
Figure 10. Analytical and numerical $\mathcal{L}^{-1}$-transformation of the function $\dot{\varepsilon}^0(t)$

The second curve drawn in this diagram represents the result of the numerical inverse LAPLACE-CARSON transformation which is applied to discrete values of $\varepsilon^{0*}(\tau, s)$. While there is a good agreement between numerical and analytical results for $t < 1.5$, significant deviations are observed for $t > 1.5$. The reason is, that the basis function of this numerical algorithm can not represent such a discontinuity.

As pointed out in Section 4.3, one basic motivation for the development of this homogenization procedure is to attain a reduced computational effort compared to the FE^2-method. In order to evaluate this time advantage, the same RVE as described in this Section is used for a FE^2-computation. Therefore, a single volume element is representing the macroscopic model where the boundary conditions are derived from the uni-axial strain function (24). The time increments Δt_i required for a single macroscopic integration point are recorded for each deformation step i. Figure 11 shows a comparison of Δt_i between FE^2-method and affine homogenization.
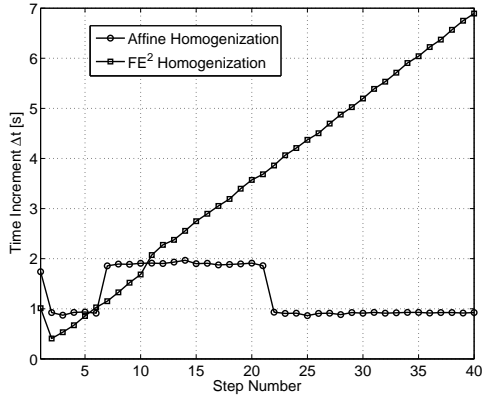
Figure 11. Time increment Δt
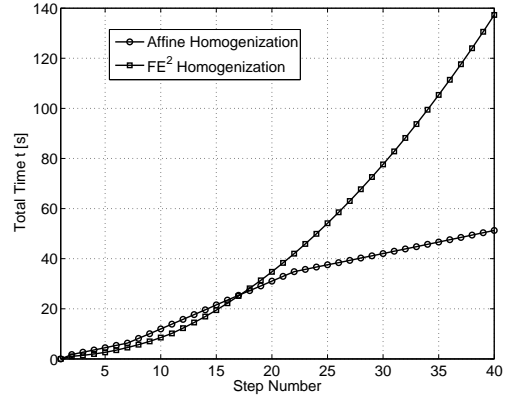
Figure 12. Total time t

In both cases, the first time increment Δt_1 is larger than the following one which is caused by reading and preparation of input data. All subsequent time increments of the affine homogenization are nearly constant within three ranges. Looking at the material behavior at each step, it can be recognized, that a visco-elastic step requires $\Delta t \approx 1\,\mathrm{s}$. Due to the additional iteration loops for a visco-plastic step, the time increment increases to $\Delta t \approx 2\,\mathrm{s}$. Unlike the affine homogenization, the size of Δt_i with $i > 1$ is rising constantly for the FE^2-method. From this follows that the character of the total time function is quadratic, which can be recognized in Figure 12. The partially linear curve of the affine homogenization verifies the improved computational efficiency since the total time at step 40 of the FE^2-computation is reduced by a factor of 2.69 from 137 s to 51 s.

This example presented here proves the possibility to simulate a viscoplastic material behavior as proposed in Section 4.3 and the computational efficiency. However, further enhancements are required. On the one hand, the accuracy of the numerical LAPLACE-CARSON transformation needs to be improved. On the other hand, the amount of data to be stored during the computation have to be reduced in order to enhance the efficiency of this homogenization procedure.

6 Summary and outlook

This study shows two possibilities to combine formulations developed in conjunction with analytical models and the numerical homogenization method based on the HILL-MANDEL condition. For each approach, the LAPLACE-CARSON transformation is used. In the case of a micro structure where the material behavior of all constituents are either linear viscoelastic or pure elastic, a closed form of effective constitutive equations can be computed. These are assigned to the elements of a FE-model representing a macroscopic structure. In comparison to analytical models, this method is not restricted to a specific type of heterogeneity and with respect to the FE^2-method, we have improved the numerical efficiency significantly.

The second approach combines the numerical homogenization method with the affine formulation. Therefor, we have introduced a new algorithm where the first explicit cycle provides an approximation based on the previously obtained solution. If necessary, the subsequent implicit cycles adjust the result according to the nonlinear material behavior at the micro scale. With the application to a homogeneous RVE, this procedure has been proven to be suitable for the simulation of viscoplastic material behavior. However, this example has shown that further improvements are required. One problem is related to the numerical inverse LAPLACE-CARSON transformation. An enhanced algorithm which can handle the specific character of the functions occurring in this affine formulation could improve the homogenized results significantly. A second problem concerns the large amount of data. Although there is less computational effort compared to the FE^2-method, the numerical implementation of the homogenization method based on the affine formulation requires the storage and arrangement of microscopic state variables as well as other quantities for each RVE and all finite elements of the RVE. In view of a structural FE-model where the macroscopic stress and tangent stiffness is computed by such affine homogenization method, the demand on memory is growing extensively. Thus, a smaller number of required data could increase the efficiency of the homogenization algorithm.

Acknowledgments

Appendix A Numerical LAPLACE-CARSON inversion

The numerical LAPLACE-CARSON transformation used here is adapted from the collocation method proposed by Schapery (1967). Thereby it is assumed, that the solution $f(t)$ can be approximated by a sum of a linear function and a finite DIRICHLET series from what follows

$$f(t) = A + Bt + \sum_{j=1}^{n_{max}} b_j(1 - e^{-\frac{t}{\tau_j}}) \circ\!\!-\!\!\bullet\ f^*(s) = A + \frac{B}{s} + \sum_{j=1}^{n_{max}} b_j \frac{1}{1 + \tau_j s} \quad , \tag{26}$$

where A, B and b_j are constants. In order to identify these parameters, limit values of the function either in time or image domain can be used. Then the values of A and B are given by

$$\begin{aligned} A &= \lim_{s \to +\infty} f^*(s) = \lim_{t \to 0} f(t) \quad \text{and} \\ B &= \lim_{s \to 0} s f^*(s) = \lim_{t \to +\infty} \frac{f(t)}{t} \quad . \end{aligned} \tag{27}$$

The remaining unknown parameters b_j can be obtained by solving the linear system of equations

$$f^*(s_l) - A - \frac{B}{s_l} = D_{lj}b_j \quad \text{with} \quad D_{lj} = \frac{1}{1 + \frac{\tau_j}{\tau_l}} \quad , \tag{28}$$

where the relaxation times are defined by $\tau_l = \frac{1}{s_l}$.

Appendix B Affine formulation adapted to Perzyna model

Details to the derivation of the affine formulation can be found in Masson and Zaoui (1999) and Pierard (2006). In order to simplify the notation, the evaluation time τ specified for tensors $\mathbf{m}$, $\mathbf{n}$, $\mathbf{p}$ and q is omitted in this Section.

Referring to the viscoplastic material law described in Section 4.1, the compliance tensor used in equation (20) is defined by

$$\mathbf{S}_\tau(\tau, t) := \mathbf{S} + \mathbf{m}\, t - \frac{1}{q} \left[t + \frac{1}{q}(1 - \mathrm{e}^{tq}) \right] \mathbf{n} \otimes \mathbf{p} \quad . \tag{29}$$

Additionally, the eigenstrain rate $\dot{\varepsilon}^0(\tau, t)$ is given by

$$\dot{\varepsilon}^0(\tau, t) := \dot{\varepsilon}^{vp}(t_n) - \mathbf{m} : \boldsymbol{\sigma}(t_n) + \mathbf{n}\,\hat{\alpha}(\tau, t) + \dot{\mathbf{e}}(\tau, t)\left[1 - H(t - t_n)\right] + \hat{\varepsilon}^0(\tau, t, \boldsymbol{\sigma}(0)) \tag{30}$$

where the following definitions are used

$$
\begin{aligned}
\dot{\mathbf{e}}(\tau, t) &:= \dot{\varepsilon}^{vp}(t) - \dot{\varepsilon}^{vp}(t_n) - \mathbf{m} : [\boldsymbol{\sigma}(t) - \boldsymbol{\sigma}(t_n)] - \mathbf{n}\left[\hat{\alpha}(\tau, t) + q \int_0^t \mathrm{e}^{t-u}\mathbf{p} : \boldsymbol{\sigma}(u)du \right], \\
\hat{\varepsilon}^0(\tau, t, \boldsymbol{\sigma}(0)) &:= \left[\mathbf{m} - \frac{1}{q}\,\mathbf{n} \otimes \mathbf{p}\,(1 - \mathrm{e}^{tq})\right] : \boldsymbol{\sigma}(0) \quad , \\
\hat{\alpha}(\tau, t) &:= \frac{1}{q}\left(\mathrm{e}^{(t-t_n)q} - 1\right)(\dot{\alpha}(t_n) - \mathbf{p} : \boldsymbol{\sigma}(t_n)) - \int_0^{t_n} \mathrm{e}^{(t-u)q}\mathbf{p} : \boldsymbol{\sigma}(u)du .
\end{aligned}
\tag{31}
$$

The HEAVISIDE step function $H(x) = \lim_{v \to x-}((|v|/v + 1)/2)$ is employed in equation (30).
Referring to equation (21), the LAPLACE-CARSON transform of the linearized constitutive law uses the definition of a compliance-like tensor

$$\mathbf{S}_\tau^*(\tau, s) := \mathbf{S} + \frac{1}{s}\mathbf{m} + \frac{1}{s(s-q)}\mathbf{n} \otimes \mathbf{p} \tag{32}$$

and a eigenstrain

$$
\begin{aligned}
\varepsilon^{0*}(\tau, s) &:= \dot{\varepsilon}^{vp}(\tau)\mathrm{e}^{-s\tau} + s \int_0^\tau \dot{\varepsilon}^{vp}(u)\mathrm{e}^{-su}du - s\,\mathbf{m} : \int_0^\tau \boldsymbol{\sigma}(u)\mathrm{e}^{-su}du - \mathbf{m} : \boldsymbol{\sigma}(\tau)\mathrm{e}^{-s\tau} - \ldots \\
&\ldots \quad -\frac{\mathrm{e}^{-s\tau}}{q-s}(\dot{\alpha}(\tau) - \mathbf{p} : \boldsymbol{\sigma}(\tau))\,\mathbf{n} + \frac{s}{q+s}\mathbf{n} : \mathbf{1}\int_0^\tau \boldsymbol{\sigma}(u)\mathrm{e}^{-su}du + \hat{\varepsilon}^{0*}(\tau, t, \boldsymbol{\sigma}(0))
\end{aligned}
\tag{33}
$$

with

$$\hat{\varepsilon}^{0*}(\tau, t, \boldsymbol{\sigma}(0)) := \left(\mathbf{m} - \frac{1}{q-s}\,\mathbf{n} \otimes \mathbf{p}\right) : \boldsymbol{\sigma}(0) \quad . \tag{34}$$

References

Abaqus: *User Subroutines Reference Manual*. Dassault Systmes Simulia Corp., Providence, RI, USA (2008), Version 6.8.

Alfrey, T.: Non-homogeneous stresses in visco-elastic media. *Quarterly of Applied Mathematics*, 2, (1944), 113–119.

Carter, W.; Cox, B.; Fleck, N.: A binary model of textile composites - I. Formulation. *Acta. metall. mater.*, 42, 10, (1994), 3463–3479.

Castañeda, P. P.: Exact second-order estimates for the effective mechanical properties of nonlinear composite materials. *Journal of the Mechanics and Physics of Solids*, 44, 6, (1996), 827–862.

Haasemann, G.: *Effektive mechanische Eigenschaften von Verbundwerkstoffen mit Biaxialgestrickverstärkung*. Ph.D. thesis, TU Dresden (2008), published by TUDpress, ISBN: 978-3-941298-01-9.

Haasemann, G.; Kästner, M.; Ulbricht, V.: Multi-scale modelling and simulation of textile reinforced materials. *CMC - Computers, Material & Continua*, 3, 3, (2006), 131–146.

Haasemann, G.; Kästner, M.; Ulbricht, V.: A new modelling approach based on binary model and x-fem to investigate the mechanical behaviour of textile reinforced composites. *CMES - Computer Modeling in Engineering & Sciences*, 42, 1, (2009), 35–57.

Hill, R.: Elastic properties of reinforced solids: Some theoretical principles. *Journal of the Mechanics and Physics of Solids*, 11, 5, (1963), 357–372.

Hill, R.: A self-consistent mechanics of composite materials. *Journal of the Mechanics and Physics of Solids*, 13, 4, (1965), 213–222.

Hill, R.: The essential structure of constitutive laws for metal composites and polycrystals. *Journal of the Mechanics and Physics of Solids*, 15, 2, (1967), 79–95.

Kaliske, M.: A formulation of elasticity and viscoelasticity for fibre reinforced material at small and finite strains. *Computer Methods in Applied Mechanics and Engineering*, 185, 2-4, (2000), 225 – 243.

Kouznetsova, V.: *Computational homogenisation for the multi-scale analysis of multi-phase materials*. Ph.D. thesis, TU Eindhoven (2002).

Mandel, J.: Contribution théorique à l'étude de l'écrouissage et des lois de l'écoulement plastique. In: *11th International Congress on Applied Mechanics*, page 502509, Springer, Berlin (1964).

Masson, R.; Zaoui, A.: Self-consistent estimates for the rate-dependent elastoplastic behaviour of polycrystalline materials. *Journal of the Mechanics and Physics of Solids*, 47, 7, (1999), 1543–1568.

Miehe, C.; Koch, A.: Computational micro-to-macro transitions of discretized microstructures undergoing small strains. *Arch. Appl. Mech.*, 72, (2002), 300–317.

Mori, T.; Tanaka, K.: Average stress in matrix and average elastic energy of materials with misfitting inclusions. *Acta Metallurgica*, 21, 5, (1973), 571–574.

Nemat-Nasser, S.; Hori, M.: *Micromechanics: Overall Properties of Heterogeneous Materials*. North-Holland, 1st edn. (1993).

Perzyna, P.: The constitutive equations for rate sensitive plastic materials. *Quarterly of Applied Mathematics*, 20, (1963), 321–332.

Pierard, O.: *Micromechanics of inclusion-reinforced composites in elasto-plasticity and elasto-viscoplasticity:modeling and computation*. Ph.D. thesis, Université Catholique de Louvain (2006).

Pierard, O.; Doghri, I.: An enhanced affine formulation and the corresponding numerical algorithms for the mean-field homogenization of elasto-viscoplastic composites. *International Journal of Plasticity*, 22, 1, (2006), 131–157.

Pierard, O.; Friebel, C.; Doghri, I.: Mean-field homogenization of multi-phase thermo-elastic composites: a general framework and its validation. *Composites Science and Technology*, 64, 10-11, (2004), 1587–1603.

Schapery, R.: Stress analysis of viscoelastic composite materials. *Journal of Composite Materials*, 1, 3, (1967), 228–267.

Takano, N.; Zako, M.; Kikuchi, N.: Stress analysis of sandwich plate by the homogenization method. *Materials Science Research International*, 1, 2, (1995), 82–88.

Address: Dr.-Ing. Georg Haasemann and Prof. Dr.-Ing. habil. Volker Ulbricht, Institut für Festkörpermechanik (Maschinenwesen), Technische Universität Dresden, 01062 Dresden.
email: georg.haasemann@tu-dresden.de; volker.ulbricht@tu-dresden.de .